



University of Dundee

Driving E3 Ligase Substrate Specificity for Targeted Protein Degradation

Cowan, Angus D.; Ciulli, Alessio

Published in:
Annual Review of Biochemistry

DOI:
[10.1146/annurev-biochem-032620-104421](https://doi.org/10.1146/annurev-biochem-032620-104421)

Publication date:
2022

Document Version
Early version, also known as pre-print

[Link to publication in Discovery Research Portal](#)

Citation for published version (APA):
Cowan, A. D., & Ciulli, A. (2022). Driving E3 Ligase Substrate Specificity for Targeted Protein Degradation: Lessons from Nature and the Laboratory. *Annual Review of Biochemistry*, 8(27), 23.1-25.25.
<https://doi.org/10.1146/annurev-biochem-032620-104421>

General rights

Copyright and moral rights for the publications made accessible in Discovery Research Portal are retained by the authors and/or other copyright owners and it is a condition of accessing publications that users recognise and abide by the legal requirements associated with these rights.

- Users may download and print one copy of any publication from Discovery Research Portal for the purpose of private study or research.
- You may not further distribute the material or use it for any profit-making activity or commercial gain.
- You may freely distribute the URL identifying the publication in the public portal.

Take down policy

If you believe that this document breaches copyright please contact us providing details, and we will remove access to the work immediately and investigate your claim.

Driving E3 Ligase Substrate Specificity for Targeted Protein Degradation: Lessons from Nature and the Laboratory

Angus D Cowan¹, ORCID: 0000-0002-9702-7319, email: acowan001@dundee.ac.uk

Alessio Ciulli¹, ORCID: 0000-0002-8654-1670, email: a.ciulli@dundee.ac.uk

¹Centre for Targeted Protein Degradation, School of Life Sciences, University of Dundee, Dow Street, Dundee, DD1 5EH, United Kingdom.

Keywords: Targeted Protein Degradation, E3 Ligase, PROTAC, Molecular Glue, Ubiquitin Proteasome System

Abstract

Directed degradation of protein targets with proximity-inducing molecules that co-opt the cellular degradation machinery is advancing in leaps and bounds, and diverse modalities are emerging. The most used and well-studied approach is to hijack E3 ligases of the ubiquitin-proteasome system. E3 ligases use specific molecular recognition to determine which proteins in the cell are ubiquitinated and degraded. This review focuses on the structural determinants of E3 ligase recruitment of natural substrates, and of neo-substrates through monovalent molecular glues and bivalent PROteolysis TARgeting Chimeras (PROTACs). We use structures to illustrate the different types of substrate recognition and assess the basis for neo-protein-protein interactions in ternary complex structures. The emerging structural and mechanistic complexity is reflective of the diverse physiological roles of protein ubiquitination. This molecular insight is also guiding the application of structure-based design approaches to the development of new and existing degraders as chemical tools and therapeutics.

Introduction

Protein homeostasis in cells comprises the many systems involved in maintaining a functional and dynamically responsive proteome. Along with protein synthesis, folding and trafficking, molecular pathways that degrade proteins are essential for maintaining protein homeostasis. The ubiquitin-proteasome system (UPS) is one of the major pathways responsible for degrading intracellular protein targets. Through the UPS, proteins are tagged for degradation by a small 8 kDa protein that is highly conserved in eukaryotes called ubiquitin. Three groups of enzymes are responsible for the priming and eventual ligation of ubiquitin primarily to a lysine residue on a substrate protein. Ubiquitin is first activated in an ATP-dependent manner by an E1 enzyme, to which it becomes covalently attached. The E1 transfers ubiquitin to an E2 enzyme via a trans-thiolation reaction. Finally, covalent ligation of the C-terminus of ubiquitin to a lysine residue of a substrate protein is catalysed by an E3 ligase (1, 2).

The mechanism of substrate ubiquitination differs among the various types of E3 ligases, including Really Interesting New Gene (RING) E3s, homologous to E6-AP C-terminus (HECT) E3s, and RING-between-RING (RBR) E3s (3, 4). The RING E3 ligases, most notably the Cullin-RING ligase (CRL) multi-subunit superfamily, bring the ubiquitin-loaded E2 and the target protein into close proximity for ubiquitin transfer directly from the E2 to the substrate (5, 6). HECT E3 ligases form a thioester intermediate with ubiquitin then subsequently transfer it to the substrate (7, 8). RBR E3 ligases are a hybrid of the RING and HECT E3 mechanisms, whereby the first RING domain binds to the E2 facilitating covalent transfer of ubiquitin to the second RING domain and then ubiquitin ligation to the substrate (9). In all cases, substrate specificity in the system is determined by the E3 ligase, which binds directly to the target substrate. Following the initial ubiquitination event, the substrate-linked ubiquitin can be ubiquitinated on one of several lysine residues leading to formation of polyubiquitin chains. Polyubiquitinated targets where ubiquitin molecules are linked at Lys48 or Lys63 are recognized by the proteasome, unfolded and proteolytically degraded. Substrate recognition, ubiquitination and degradation are presented schematically in **Figure 1a**. Through the UPS, cells can rapidly respond to various stimuli to degrade or cease degradation of myriad proteins within the cell. In addition to linear chains, there are also branched ubiquitin chains that have recently been implicated to play a role in efficient signalling for proteasomal degradation (10, 11). Alternative types of ubiquitin chains beyond K48- and K63-linked can also be built by E3 ligases,

upon linkages to other lysine residues on ubiquitin (K6, K11, K27, K29, and K33) or to its N-terminus (M1) (12). These tend to have non-degrading roles, so they are not considered here.

Modulation and manipulation of the crucial role that the UPS plays within cells has been explored in recent years in both chemical biology and therapeutic contexts (13, 14). Redirection of the ubiquitination machinery for targeted protein degradation (TPD) of non-native neo-substrates is an emerging pharmacological strategy for disease intervention (15, 16). Early exploration of TPD by Howley and colleagues involved fusing the human papillomavirus protein E7 and the Cullin-RING ligase (CRL) substrate receptor F-Box protein β -TrCP with the object of eliminating the E7 binding partner retinoblastoma protein (17). The field of TPD blossomed further with the development of heterobifunctional peptidic molecules by the groups of Crews and Deshaies. In early proof-of-concept work, one end of the bifunctional molecule consisted of the natural peptide ligand for the β -TrCP E3 ligase substrate receptor and the other the small molecule ovalicin, a ligand for methionine aminopeptidase (MetAP)-2 (18). These heterobifunctional molecules were termed PROteolysis TARgeting Chimeras (PROTACs), bringing the two proteins into proximity and leading to MetAP-2 ubiquitination and degradation in *Xenopus* egg extracts. The initial PROTACs were only used *ex cellulo* or required microinjection into cells. Subsequent work developed cell permeable PROTACs consisting of a hypoxia-inducible factor alpha (HIF1 α) peptide to bind and recruit the E3 ligase CRL2^{VHL} (with a polyarginine tag for cell permeability) fused to either an artificial ligand that binds mutant FKBP12 protein or a dihydrotestosterone (DHT) derivative that binds the androgen receptor (19). Treatment of cells with these PROTACs led to target protein degradation, highlighting the potential of such molecules as both biological tools and therapeutics. A decade later, non-peptidic ligands for E3 ligases were developed, including for the CRL2 substrate receptor VHL and the CRL4 substrate receptor Cereblon (CRBN). These ligands enabled the generation of much-improved PROTACs with potent and specific degradation activities effective in cells and animal models (20-24). Almost two decades on from their pioneering introduction, PROTACs have entered the clinic (25) and are primed to deliver on their therapeutic promise. A schematic representation of the mechanism of action of a typical PROTAC is presented in **Figure 1b**.

Two components determine substrate specificity for the ubiquitination of natural and non-natural substrates of E3 ligases. First, the substrate must contain a motif that be recognized and engaged by the E3, and second, a lysine residue to which ubiquitin will be attached must be present and accessible to the E3 on the substrate. These two essential elements collectively represent a degron: the minimal recognition motif required to target a protein for degradation by the UPS. This review will focus on the first component, the molecular recognition of substrate and neo-substrate motifs by E3 ligases, in nature and in the context of chemical/pharmacological approaches to TPD, respectively. Examples will be provided where the structural determinants are known. This review will not discuss fusion protein- and antibody-based TPD systems which have been expertly reviewed elsewhere (26, 27).

Substrate ubiquitination and degradation must be dynamic to respond quickly to diverse intracellular and extracellular stimuli. Here, we broadly divide E3 binding and recognition of substrate degrons into three distinct types:

- **Type 1.** Recognition of a constitutive degron in the native fold of the substrate by a natively folded E3 ligase.
- **Type 2.** Recognition of a degron that arises from post-translational modification (PTM) of the substrate.
- **Type 3.** PTM of the E3 resulting in recognition of a substrate degron.

Type 2 and 3 modification, examples of which will be given later, can be further divided into interfacial or allosteric modifications and may be covalent or non-covalent, or involve a proteolytic cleavage event. A schematic representation of type 1, type 2 and type 3 substrate recognition is presented in **Figure 2**. General modifications that regulate E3 ligase function, such as NEDDylation of CRLs, and other types of substrate recognition such as regulation by substrate receptor localization have been reviewed in a recent issue of Annual Reviews of Biochemistry (28) and will not be discussed here.

Many hundreds of E3 ligases recognize myriad diverse substrate proteins, sometimes a single protein and sometimes whole families with conserved structural features. The molecular determinants of recognition have been investigated through structural methods, primarily by X-ray crystallography and increasingly by cryo-electron microscopy (cryo-EM). The next section will discuss protein structures that have provided insights into the recognition process.

Substrate Recognition in Nature

In type 1 substrate recognition, substrates may be constitutively degraded until inhibitory feedback mechanisms are engaged. Such is the case for degradation of dishevelled proteins (DVL)1-3, where the BTB CRL3^{KLHL12} E3 ligase constitutively recognizes and ubiquitinates DVL1-3 (29). Inhibition of CRL3^{KLHL12} by NRX and PLEKHA4 allows progression of WNT signaling (30, 31). X-ray crystal structures of the CRL3 substrate receptor Kelch-like protein 12 (KLHL12) in complex with different DVL substrate peptides were reported recently by two groups (32, 33). The DVL1 structure reveal that the proline-rich PGXPP recognition motif in the peptide bound to the hydrophobic pocket at the centre of the Kelch β -propeller adopts a U-shaped type II β -turn (34). The turn is stabilised by an intramolecular hydrogen bond between the backbone carbonyl of Pro657 and the backbone amine of Gly660 (residues *i* and *i*+3 in β -turn nomenclature, respectively) (**Figure 3a**). Bulky hydrophobic side chains in the KLHL12 barrel interact with the pyrrolidine rings of proline residues P658, P657 and P661 in the DVL1 peptide, and an intermolecular hydrogen bond is formed between the backbone carbonyl of Pro658 in DVL1 and the hydroxyl group of Tyr512 in KLHL12 (**Figure 3a**). Other structurally characterised examples of type I substrate recognition can be found in the X-ray crystals structures of the CRL3 substrate receptor KLHL20 in complex with a peptide from substrate DAPK1 (35), the CRL3 substrate receptor SPOP in complex with several substrate peptides (36, 37), and the cryo-EM structure of CRL5^{ASB9} in complex with its substrate Creatine Kinase brain-type (38).

The N- and C-termini of proteins can act as recognition motifs for N- and C- degron pathways, respectively (39, 40). N- and C-degrons may constitute either unmodified (type 1 substrate recognition) or modified (type 2 substrate recognition) N- or C-termini. Type 2 recognition may involve a cleavage event that exposes neo-N- or neo-C-termini degrons, and/or modification of terminal residues (e.g., N-terminal acetylation). Different N- and C-terminal residues and their modifications thereby dictate the half-lives on the protein in which they reside through the UPS. An example of a type 2 N-degron can be found in the yeast glucose-induced degradation (GID) protein complex that degrades gluconeogenic enzymes when glucose-starved yeast are transitioned glucose-replete conditions (41, 42). The substrate recognition subunit GID4 recognises the N-terminal proline (N-Pro) residue of gluconeogenic enzymes that is exposed through co-translational proteolytic removal of the initiator methionine by MetAPs (43, 44). The structure of the substrate receptor subunit GID4 was solved in complex with a tetrapeptide containing an N-Pro, showing a tight interaction network of hydrogen bonds between backbone atoms of the tetrapeptide and backbone and sidechain atoms at the centre of the GID4 β barrel (**Figure 3b**) (45). The rigidity and increased basicity of proline in comparison to other amino acids explains why no other amino acids that are exposed by MetAP cleavage (G, A, S, C, P, T and V (44)) are tolerated in this position (43). An exquisite hydrogen and ionic bonding network centred around the proline residue, involving a

hydrogen bond between the proline backbone carbonyl and the side chain of Gln132 of GID4, a hydrogen bond between the pyrrolidine nitrogen and the hydroxyl group of Tyr258 (which is in turn positioned by another H-bond with Gln132), and finally a salt bridge between the pyrrolidine nitrogen and carboxyl group of Glu237 (**Figure 3b**).

In addition to responses to environmental stimuli, some E3 ligases are involved in protein quality control. The Cul2 substrate receptor Kelch domain-containing protein 2 (KLHDC2) recognises and ubiquitinates polypeptides terminating in a C-terminal diglycine motif (46, 47). The motif is found in some full-length proteins, but also in early-terminated fragments of selenoproteins SelK and SelS and the proteolytically generated N-terminal fragment of the deubiquitinating enzyme USP1. The crystal structure of the KLHDC2 in complex with a SelK substrate peptide demonstrates an intricate hydrogen and ionic bonding network that is structurally licensed by the flexibility of the diglycine motif (**Figure 3c**) (47).

Beyond proteolytic cleavage, type 2 substrate recognition occurs with many other PTM-generated degrons. The suppressor of cytokine signalling (SOCS) protein family inhibit cytokine signalling through the JAK-STAT pathway through several mechanisms, including acting as substrate receptors for Cul5-ElonginB/C -type Cullin RING E3 ligases. They contain a SOCS box to recruit adaptor proteins Elogins B and C and Cul5, as well as a Src-homology 2 (SH2) domain that binds to peptide motifs containing phosphorylated tyrosine residues in substrates. In addition, SOCS1 and SOCS3 possess a kinase inhibitory region (KIR), which inhibits the kinase activity of certain Janus kinases (JAKs) by blocking their substrate binding groove (48, 49). Structures of SOCS family SH2 domains, including SOCS1, SOCS2, SOCS3 and SOCS6, have been solved in complex with substrate or binding partner peptides (48-51). **Figure 3d** shows the SOCS2 SH2 domain in complex with a phosphorylated peptide from the erythropoietin receptor EpoR, with the characteristic deep basic pocket lined by arginine and serine residues for phosphor group binding (51).

In conditions of normal oxygen levels, the transcription factor HIF1 α is *trans*-4-prolyl hydroxylated on proline residues 402 and 564 (52, 53). In another example of type 2 substrate recognition resulting from covalent PTM, the CRL2^{VHL} E3 ligase binds the hydroxylated P564 residue leading to constitutive ubiquitination and degradation. Under hypoxic conditions, HIF1 α escapes proline hydroxylation, is therefore no longer degraded by CRL2^{VHL}, and can rapidly accumulate in the nucleus to activate expression of hypoxia response genes. The structure of the hydroxylated HIF1 α peptide bound to VHL reveals how specificity for the hydroxylated form of HIF1 α is achieved through a hydrogen bonding network between S111 and H115 of VHL and the 4-hydroxyl group of the hydroxylated P564 (HyP564) sidechain of HIF1 α , as HyP564 adopts its preferred C4-exo ring pucker in order to fit snugly within the VHL binding pocket (**Figure 3e**) (54, 55). While small molecule targeting of ubiquitous and charged interactions in phosphopeptide binding proteins such as SOCS2 have proved difficult, the unique and relatively specific features of post-translationally modified residues such as the hydroxylated HIF1 α peptide inspired structure-guided design of small molecule binders such as the VHL inhibitors VH032 and VH298 (56, 57). These VHL ligands will be discussed further in the PROTAC section of this review.

Both type 2 and type 3 substrate recognition can also result from non-covalent modifications of protein structure through metabolite and small molecule binding. In another example of oxygen and also iron sensing, a combination of type 2 and type 3 substrate recognition occurs in the case of CRL1^{FBXL5}-mediated ubiquitination and degradation of iron regulatory protein 2 (IRP2) in iron- and oxygen-replete cells (58-64). Type 2 non-covalent allosteric recognition is dictated by iron-sulfur [4Fe4S] cluster insertion into IRP2, where cluster insertion induces a rotation of IRP domain III towards domain IV, sterically hindering the interaction with the substrate receptor FBXL5 (65). Type 3 non-covalent allosteric recognition includes both oxygen- and iron-dependent modification of the

FBXL5 fold. Both the N-terminal hemerythrin-like (Hr) domain and a C-terminal leucine-rich repeat (LRR) domain bind iron, either as a diiron center or iron-sulfur [2Fe2S] cluster, respectively (65, 66). The conformation of the LRR domain is also coupled cellular oxygen levels through the oxidation state of an iron-sulfur [2Fe2S] cluster (65). Four cysteine residues in the C-terminal loop region of FBXL5 fold around the oxidised form of the [2Fe2S] cluster, placing the “interface loop” in a conformation that can engage domain IV of the substrate IRP2 (**Figure 3f**), leading to its ubiquitination and degradation (65). Upon reduction of the [2Fe2S]²⁺ cluster to [2Fe2S]⁺ in conditions of hypoxia, FBXL5 binding to IRP2 is impaired, likely due to the interface loop adopting a conformation incompatible with IRP2 binding (65).

Certain plant hormone systems rely on type 3 non-covalent interfacial substrate recognition, with binding of the phytohormones auxin and jasmonate to their cognate CRL1 E3 ligase substrate receptors transport inhibitor response 1 (TIR1) and coronatine-insensitive 1 (COI1), respectively. In addition, type 3 non-covalent allosteric recognition also occurs with binding of inositol polyphosphates (InsP) to both substrate receptors, influencing E3 ligase activity (67, 68). Hormone binding enables substrate recognition and ubiquitination; for TIR1 the AUX/IAA repressor proteins; and for COI1 the JAZ transcription factor. The structure of *Arabidopsis thaliana* TIR1 in complex with InsP₆, auxin and a substrate peptide from UAX/IAA repressor protein IAA7 revealed auxin bound to a pocket on TIR1, creating a new molecular surface to which the IAA7 bound (**Figure 3g**) (67). Auxin thereby acts as a molecular glue degrader, holding the two proteins together such that ubiquitination of the substrate is dependent on the presence of Auxin (67). The next section of this review will cover synthetic molecular glue degraders created in the laboratory and how they are able to bridge E3 ligases to neo-substrates that are not normally engaged in the absence of the chemical compound.

Neo-substrate Recognition in Targeted Protein Degradation

Molecular Glues

A small but growing number of synthetic molecular glue degraders induce *de novo* protein-protein interactions (PPIs) to facilitate ubiquitination of neo-substrates in a manner reminiscent of the auxin/jasmonate plant hormone systems. Historically, these molecules have been discovered serendipitously through phenotypic screening campaigns, with their mode of action being elucidated later (69, 70). A schematic representation of the mechanism of action of a typical molecular glue is presented in **Figure 1c**.

The first and most infamous example of a synthetic molecules shown to function as molecular glue degraders are phthalimide-based immunomodulatory drugs (IMiDs). Thalidomide, the first-in-class phthalimide drug approved for use in the 1950s, caused severe birth defects when administered as a sedative to pregnant women. It was subsequently determined to be a potent teratogen (71). Though rapidly withdrawn from the market and banned for human use, thalidomide, and its analogues pomalidomide and lenalidomide, have since been found to be efficacious in treating select diseases, first for leprosy and later for some hematological cancers. The cellular “target” of IMiDs was discovered identified to be CRBN, some six decades after thalidomide was first prescribed (72). Co-crystal structures of IMiDs bound to CRBN confirmed target engagement and revealed the binding site on the substrate recognition subunit of the CRL4^{CRBN} E3 ligase (73, 74). The mechanism of action was later determined to involve type 3 non-covalent interfacial substrate recognition, where phthalimide-bound CRBN recruits neo-substrate zinc finger transcription factors Ikaros and Aiolos for ubiquitination and subsequent proteasomal degradation (75, 76). Other neo-substrates of IMiDs have since been identified with a common β-hairpin structural motif. The recent structure of the thalidomide metabolite 5-hydroxythalidomide (5HT) in complex with SALL4 (**Figure 4a**) is

especially notable, as degradation of SALL4 is responsible for the teratogenicity of the drug (77). As with the auxin structure, 5HT binds to a pocket on CRBN to create a new molecular surface that recruits the zinc finger (ZF)2 domain of SALL4 through its β -hairpin (77). Interestingly, when compared the thalidomide, the metabolite 5HT displays altered neo-substrate specificity that can be rationalised by structural comparison of the two drugs in complex with CRBN and SALL4 ZF2 (77). These findings suggest small modifications to molecular glue degraders could tune specificity and may even lead to recruitment of additional neo-substrates. Many proteins are known or predicted to contain zinc fingers and a structurally conserved β -hairpin loop as potential structural degron, and so classify as putative substrates of IMiD-bound CRBN (78).

The anti-cancer aryl-sulfonamide compounds, including indisulam and E7820, exert their anti-proliferative effects by acting as molecular glues. The compounds recruit RNA-binding proteins (RBM), specifically RBM39 and to a lesser extent RBM23 to the CRL4 substrate receptor DDB1- and CUL4-associated factor (DCAF)15, with the antiproliferative effect mediated through RBM39 ubiquitination and degradation (79, 80). Three papers revealed the structural determinants of aryl-sulfonamide compound binding and gluing (81-83), and the structure of indisulam in complex with DCAF15 and RBM39 is presented in **Figure 4b** [the CRL4 adaptor protein DNA damage-binding protein 1 (DDB1) and accessory protein DET1- and DDB1-associated protein 1 (DDA) were also part of the complex but are not depicted]. Although the complexes formed between aryl-sulfonamide compounds, DCAF15 and RBM39 are stable and long-lived, the compounds alone have non-detectable or very low affinity for DCAF15 and RBM39 in binary interactions. This phenomenon likely arises from the large neo-protein-protein interface between DCAF15 and RBM39 on top of the more minor but essential interactions the glues contribute. **Table 1** shows the buried surface area contributions of each component to the overall assembly for this structure and for other molecular glue and PROTAC ternary structures covered in this review. An interesting comparison can be made to the CRBN:5HT:SALL4 complex, where the binary K_D between the *S* enantiomer of 5HT and CRBN is $0.76 \pm 0.20 \mu\text{M}$. The CRBN:SALL4 interface has an interface area of 479.1 \AA^2 with a Δ^iG of -0.2 kcal/mol , Δ^iG P-value of 0.670, 7 hydrogen bonds and no salt bridges as calculated using PISA. (See the PDBePISA webserver for definition of Δ^iG and Δ^iG P-values, and note that all further interface analyses in this review are performed with PISA) (84, 85). These values are similar to those seen in crystal contacts, whereas interface between DCAF15 and RBM39 is more extensive and reminiscent of a native protein-protein interface. The DCAF15:RBM39 interface encompasses area of 1209.8 \AA^2 ; the surface area has many hydrophobic interactions, which contribute a Δ^iG of -8.0 kcal/mol , Δ^iG P-value of 0.501, and 11 hydrogen bond and 7 salt bridges (see **Table S1** for detailed PISA-generated statistics of interfaces and assemblies in the ternary structures induced by molecular glues and PROTACs). While IMiD-induced substrate recognition can be categorised as type 3 as defined above, sulfonamide-induced substrate recognition is likely a hybrid of both type 2 and type 3 substrate recognition, where both the neo-substrate and E3 ligase interfacial surfaces are non-covalently modified by the aryl-sulfonamides.

Though the majority of currently known molecular glue degraders discovered through phenotypic screens have been identified retrospectively, targeted screens to find glues that enhance E3 ligase-substrate interactions have also yielded interesting compounds. Type 2 interfacial substrate recognition of the doubly phosphorylated phosphodegron of the oncogenic transcription factor β -catenin by its cognate E3 CRL1 ^{β -TrCP} leads to its ubiquitination and degradation (86, 87). Mutations to β -catenin or decreased levels of phosphorylation can weaken the interaction with CRL1 ^{β -TrCP}, stabilising β -catenin and leading to constitutive WNT signalling in most colorectal cancers (88, 89). A targeted screen to stabilise the interaction between monophosphorylated mutant β -catenin and CRL1 ^{β -TrCP} identified a lead that was improved by structure-guided design. This study resulted in small molecule glue compounds that enhanced affinity for a monophosphorylated pSer33 β -catenin peptide by >10,000-fold (90). The crystal structure of Skp1- β -TrCP in complex with the

monophosphorylated pSer33 β -catenin peptide and the glue NRX-2663 shows the compound filling the binding pocket normally occupied by the second phosphor group at Ser37 of the doubly phosphorylated peptide, holding the β -catenin peptide and substrate receptor β -TrCP together (**Figure 4c**) (90).

The discovery of molecular glue degraders has generally been driven through phenotypic screening searching for efficacious compounds rather than directly searching for compounds with degrader activity. A recent study set out to identify compounds with glue degrader properties by correlating drug-sensitivity data of clinical and pre-clinical drugs tested in cancer cell lines with mRNA levels of 499 E3 ligase components (91). The CRL4 substrate receptor DCAF15 was used as a proof of principle, with sensitivity of known aryl-sulfonamide degraders indisulam and tasisulam correlating with mRNA levels of DCAF15 across the drug-sensitivity dataset. The cyclin-dependent kinase (CDK) inhibitor CR8 emerged as a potential degrader through correlation of CR8 sensitivity with mRNA levels of the CRL4 adaptor DDB1. Examples of glue degraders given above involve complexation of substrates and neo-substrates directly with the substrate receptors of CRLs. Somewhat surprisingly, mRNA levels for known CRL4 substrate receptors that bind DDB1 did not correlate with sensitivity to CR8. Quantitative proteome-wide mass spectrometry revealed cyclin K was depleted in CR8-treated cells as opposed to any CDK to which CR8 binds. Instead of recruiting a neo-substrate to an E3 substrate receptor, CR8 functions through an unprecedented mechanism, whereby a CR8-bound CDK12-cyclin K complex is glued directly to the DDB1 adaptor protein. Two other groups identified and validated other compounds that glue CDK12 to DDB1 around the same time through different methods, suggesting that many compounds can function as molecular glues for the DDB1-CDK12 interaction (92, 93). The crystal structure of DDB1 in complex with CR8, CDK12 and cyclin K, shows CR8 bound to the ATP-binding pocket of CDK12 and the β -propeller C (BPC) domain of DDB1 (**Figure 4d**) (91). The PPIs between DDB1 and CDK12 are extensive. The C-lobe of CDK12 interacts with the β -propeller A (BPA) domain of DDB1, while the C-terminal tail of CDK12 binds to the cleft between the BPA and β -propeller C domains. This latter site is responsible for binding of cognate CRL4 substrate receptors such as CRBN and DCAF family proteins. Cyclin K is engaged with CDK12 distal to the interactions with DDB1, making no direct contacts with the adaptor protein. Thus, CDK12 acts as a neo-substrate-receptor, that recruits its cognate binding partner cyclin K for ubiquitination by CRL4.

A novel avenue to targeted protein degradation has recently been highlighted in the case of the oncogenic non-enzymatic transcription factor BCL6. The BCL6 inhibitor BI-3802 induces polymerisation of BCL6 into filamentous structures, acting as a molecular glue between BCL6 homodimers (94). This small molecule-mediated polymerization of BCL6 accelerates its ubiquitination by the non-Cullin E3 ligase SIAH1 that recognizes a VxP degron motif. The affinity of the SIAH1 for BCL6 is greatly enhanced in the presence of BI-3802, likely due to cooperativity from the polymerization of BCL6. This mechanism of action, which may be widely applicable to symmetrical proteins where there is potential to induce polymerization, has great therapeutic potential due to its specificity: only the target is polymerized then degraded by its cognate E3 ligase.

PROTACs

Since the 2015 studies disclosing significantly improved PROTACs based on VHL and CRBN ligands, as mentioned above, the field has witnessed an exponential growth in papers, patents, and undisclosed drug discovery programmes developing PROTAC molecules. The expanding diversity of chemistries, biological targets, and therapeutic developments of PROTACs are extensively reviewed elsewhere (95-98). Here, we will focus on structural studies that have contributed to illuminating PROTAC mechanisms of molecular recognition and mode of action.

Unlike molecular glues which are generally monovalent and bind primarily to either the neo-substrate or the E3 ligase, PROTACs are multivalent molecules that contain individual binding moieties covalently attached through a chemical linker. Each binding group can engage independently with the target neo-substrate or the E3 to be recruited; the formation of a ternary 1:1:1 complex consisting of the neo-substrate, the PROTAC and the E3 is what elicits degradation. As such, PROTACs were initially thought to work independently of PPIs and primarily by a tethering mechanism of induced proximity. In this model, ubiquitination occurs when the PROTAC tethers the neo-substrate to the E3 in close but highly flexible proximity. Structural and biophysical data have since shown that PROTACs can also function similarly to molecular glues, in that they can induce neo-PPIs between the E3 and the target protein, which contribute to the formation of a stable and cooperative ternary complexes between neo-substrate, PROTAC and E3 (99). Cooperativity (α), is defined as the ratio of dissociation constants for a given PROTAC binding to one binding partner (e.g. the neo-substrate) in the absence (binary K_D) and presence (ternary K_D) of the second binding partner (e.g. the E3 ligase) ($\alpha = K_D^{\text{binary}}/K_D^{\text{ternary}}$) (99). Cooperativity can be positive (wherein PPIs enhance ternary complex formation), non-cooperative (wherein PPIs neither enhance or inhibit ternary complex formation), or negative (wherein steric clashes and other factors inhibit ternary complex formation). The stability and positive cooperativity of ternary complexes correlates with more efficient degradation of neo-substrates where the ternary complex is productive, i.e., substrate positioning is such that a lysine residue on its surface can undergo E2-catalyzed ubiquitination (100, 101).

The first structural insight into PROTAC ternary complex formation was that of the PROTAC MZ1, a CRL2^{VHL}-recruiting degrader of the transcriptional regulator bromodomain and extraterminal domain (BET) proteins BRD2, BRD3 and BRD4 (99). BET family proteins regulate cell proliferation and cell cycle progression and have become targets of therapeutic interest in cancer, neurological disorders and inflammation (102, 103). The crystal structure of the substrate receptor VHL (complexed with adaptor proteins Elongins B and C here and in other structural examples below) bound to MZ1 and the second bromodomain (BD2) of BRD4 revealed MZ1 engaged in the expected binary binding interactions with VHL through its VH032 moiety and BRD4 BD2 through its JQ1 moiety (**Figure 5a**) (99). In addition to these protein-ligand interactions, the flexible PEG linker collapses and interacts favourably with BRD4. Both VHL and BRD4 shield parts of JQ1 and VH032, respectively, that would otherwise be solvent-exposed in the binary complexes. Due to the extensive, isoform-specific PROTAC-induced PPIs between VHL and BRD4, ternary complex formation is highly cooperative ($\alpha = 18$) and long-lived ($t_{1/2} > 2$ min), explaining the preferential degradation of BRD4 by MZ1 over the other BET proteins BRD2 and BRD3, despite the parent compound JQ1 being a pan-specific BET inhibitor (100). The structure of the ternary complex informed design of an even more selective BRD4 degrader AT1, as well as a macrocyclic PROTAC, MacroPROTAC-1, which constrains the PROTAC in its bioactive conformation (**Figure 5b**) (99, 104). The macrocyclization design strategy was shown to be effective, as MacroPROTAC-1 degradation activity was comparable to its parent non-cyclic MZ1, despite losing more than 10-fold binding affinity for the BET bromodomain due to steric clashes from the added cyclizing linker (104).

Structure-based design has also generated potent CRL2^{VHL}-recruiting degraders of another bromodomain-containing protein family: the SWI/SNF Related, Matrix Associated, Actin Dependent Regulator of Chromatin, Subfamily A (SMARCA) proteins SMARCA2 and SMARCA4 (105). After an initial round of PROTAC design and screening using a SMARCA bromodomain ligand (106, 107) and the potent VHL binder VH298 (108), PROTAC 1 was identified as a partial degrader of SMARCA2 and SMARCA4. This compound exhibited positive cooperativity ($\alpha = 4.8$) for ternary complex formation as measured by isothermal titration calorimetry. The crystal structure of the ternary complex revealed the expected binary interactions between the respective protein-binding moieties of the PROTAC and their targets, as well as PROTAC-induced PPIs between VHL and SMARCA2

bromodomain. Structure-guided optimisation of the linker to rigidify it, pick up a π -stacking interaction with VHL Y98, and increase lipophilicity led to PROTAC 2, which exhibited more favourable ternary complex formation and cellular permeability. Another pair of crystal structures of ternary complexes induced by PROTAC 2 with both SMARCA2 (**Figure 5c**) and SMARCA4 bromodomains revealed the linker π -stack with VHL Y98 had been picked up as designed, with minimal changes to the rest of the binding mode. Further linker optimisation led to ACBI1, a PROTAC with a α value of ~ 30 and a DC_{50} (half-maximal target degradation) of 6 and 11 nM for SMARCA2 and SMARCA4, respectively, an almost improvement 50-fold for SMARCA2 and 22-fold for SMARCA4 over the original PROTAC 1 (105).

The above-described studies support the formation of stable and cooperative ternary complexes as key intermediate species driving favourable and efficient protein ubiquitination. Nonetheless, positive cooperativity is not strictly required for efficient degradation of target proteins by PROTACs as was shown for both VHL-based PROTACs that degrade BET proteins (109), and with IMiD-based CRL4^{CRBN}-recruiting dBET PROTACs that degrade BRD4 (110). VHL-based MZP-type PROTAC degraders all exhibited negative cooperativity, and were poorer degraders than the MZ-type PROTACs despite being designed from BET inhibitors that had >10 -fold greater binding affinity at the BET bromodomains (109). Still, they were able to act as degraders, albeit with narrower pharmacological range and earlier onset of the hook effect (where at higher concentrations, the target and E3 binding sites become saturated leading to non-productive binary complexes(111)) compared to the MZ1 PROTAC. The CRBN-based dBET degraders exhibited varying levels of negative cooperativity with individual BRD4 bromodomains BD1 and BD2; however, their cooperativity values were still generally proportional to their cellular dBET activity. Despite negative cooperativity being indicative of unfavourability in ternary complex formation, the structures of CRBN and BRD4 BD1 complexes with several dBETs were determined. Due poor resolution (3.3 Å or lower), the dBET used was only modelled in two of the five structures reported. Comparisons of the interface and assembly properties of these and other low resolution structures with higher resolution structures in **Tables 1** and **S1** should be made with caution. The ternary structure of CRBN, dBET23 and BRD4 BD1 is presented in **Figure 5d**. Taken together, the structures reveal BRD4 BD1 binds different surfaces of CRBN depending on the dBET used, recapitulating mutagenesis data from the same study. Docking of lenalidomide-bound CRBN and JQ1-bound BRD4 BD1 was performed in the absence of degraders to look for low energy minima and potential docking poses with the shortest distance between the lenalidomide and JQ1 were used for degrader design. The resulting optimised compound using a different linker point on JQ1, ZXH-3-26, showed more selective degradation of BRD4 BD1 over other truncated BRD2, BRD3 and BRD4 bromodomains, compared to dBET6, MZ1 and dBET57, each of which degraded at least one other bromodomain.

Another structure of a ternary complex with a negatively cooperative PROTAC has recently been solved, that of a CRL2^{VHL}-recruiting BCL-X_L PROTAC degrader, PROTAC 6 (**Figure 5e**) (112). BCL-X_L is an antiapoptotic BCL-2 family protein of therapeutic interest in the treatment of many cancers (113, 114), but the use of BCL-X_L inhibitors is complicated by on-target dose-limiting thrombocytopenia because platelets depend on BCL-X_L for survival (115). Platelets express low levels of VHL, and CRL2^{VHL}-recruiting PROTACs targeting BCL-X_L circumvent the toxicity issues associated with BCL-X_L inhibition, leaving platelet populations largely intact (116). PROTAC 6 was developed using a highly selective and potent BCL-X_L inhibitor (117). Interestingly, despite the slight negative cooperativity, PROTAC 6 induces several neo-PPIs between BCL-X_L and VHL, including a salt bridge between D133 of BCL-X_L and R60 of VHL. As in the comparison of indisulam and 5HT outlined in the molecular glue section of this review, comparisons of the properties of the protein-protein interfaces between substrate receptor and neo-substrate induced by the positively cooperative MZ1 vs. the negatively cooperative PROTAC 6 provide interesting insights. Between the two copies of the complex in the asymmetric unit (ASU) of the MZ1 PROTAC structure, the BRD4:VHL interface has an average ΔG

value of -1.5 kcal/mol, average Δ^iG P-value 0.59 and also includes up to 7 hydrogen bonds and 7 salt bridges, values suggestive of a weak native PPI (84, 85). On the other hand, the protein-protein interface induced by PROTAC 6 between BCL-X_L and VHL has a positive Δ^iG value of 2.9 kcal/mol, a Δ^iG P-value of 0.849, no hydrogen bonds and 1 salt bridge, values more suggestive of a crystal contact-like interface (84, 85).

Two ternary crystal structures of a non-cooperative and an optimized positively cooperative cellular inhibitor of apoptosis 1 (CIAP1)-recruiting PROTAC degraders of Bruton's tyrosine kinase (BTK) have recently been reported. The initial structure of the non-cooperative degrader BC5P in complex with CIAP1 baculoviral-IAP repeat domain 3 (BIR3) and BTK revealed 3 PROTAC-induced ternary complexes in the ASU, all with different orientations of BTK in relation to CIAP^{BIR3} and different protein-protein interactions. As with the dBET structures, the low resolution of this structure precludes accurate analysis of the PPIs. However, manual examination of the structure reveals minimal contacts between substrate receptor and neo-substrate for two of the copies of the ternary complex in the ASU and a slightly larger interface for the third copy. The structure of the linker-optimised, positively cooperative degrader BCPyr in complex with CIAP1^{BIR3} and BTK reveals two copies of the CIAP^{BIR3}:BCPyr:BTK complex in the ASU (**Figure 5f**). The protein-protein interfaces between CIAP1^{BIR3} and BTK have an average Δ^iG value of -1.55 kcal/mol, average Δ^iG P-value 0.603 and the presence of up to 8 hydrogen bonds and 3 salt bridges, values similar to those observed for the VHL:MZ1:BRD4 complex (84, 85). Despite the increase in cooperativity when moving from BC5P to BCPyr, BC5P was a superior degrader of BTK in cellular assays. While many factors can affect cellular potency of PROTACs, including compounds' cell permeability, the similarity of the calculated properties of BC5P and BCPyr suggest the difference in potency may be due to the greater degree of flexibility in the CIAP^{BIR3}:BC5P:BTK complexes. This flexibility may allow better access of the E3 ligase to BTK lysine residues as compared to the more rigid CIAP^{BIR3}:BCPyr:BTK complex. This study and the work with dBET degraders suggest stable and rigid ternary complexes may not always lead to the most efficient degradation of target proteins, possibly due to the second requirement in a degron for a lysine residue on the target protein that is accessible to the recruited E3 ligase for ubiquitin attachment.

Positive cooperativity contributes to augment the stability of PROTAC ternary complexes, thereby enhancing the chances of cocrystallising the complex. Two final examples of positively cooperative PROTAC ternary complex structures have been reported recently. The first structure was determined as part of a large campaign of antibody-drug conjugates (ADCs) incorporating CRL2^{VHL}-recruiting, BRD4-targeting degraders that deliver the PROTACs to cells (118, 119). The structure, consisting of VHL, compound 9 and BRD4, is presented in **Figure 5g** (119). Although the authors do not report a cooperativity value for their PROTAC (compound 9), the long half-life of the ternary complex as measured by SPR is suggestive of positive cooperativity. With this in mind, it is not surprising that the protein-protein interface induced by compound 9 is more reminiscent of a weak native protein-protein interface similar to the VHL:MZ1:BRD4 complex, with a Δ^iG value of -3.6 kcal/mol, 3 hydrogen bonds and 3 salt bridges (84, 85). Still, the PROTAC induces the formation of a unique ternary complex where the orientation of the BRD4 bromodomain and VHL differs dramatically from the VHL:MZ1:BRD4 complex. These findings suggest that, at least in the context of BRD4:VHL, very different orientations of neo-substrate relative to E3 ligase can result in substrate ubiquitination.

The last structure we cover is of a CRL2^{VHL}-recruiting PROTAC degrader of focal adhesion kinase (FAK, also known as PTK2) (120), an important cancer target in solid tumours that is associated with poor clinical outcomes (121, 122). FAK-degrading PROTACs active in cellular assays had previously been reported by groups at Yale University (CRL2^{VHL}-recruiting), Boehringer Ingelheim/University of Dundee (CRL2^{VHL}- or CRL4^{CRBN}-recruiting), and Tsinghua University (CRL4^{CRBN}-recruiting) (123-125). Although some have since been shown to be active in mouse models (126-128), biophysical

characterisation of ternary complex formation and structure were lacking prior to work by Law *et al.* (120). In this study, PROTACs were designed based on the FAK inhibitor VS-4718/PND-1186 (129) and the VHL ligand (130) with different linkers. Using FRET assays to measure cooperativity, they observed positive cooperativity for all compounds. Higher cooperativity was correlated with greater potency of degradation. GSK215, with an unusually short acetamide linker, displayed the most potent degradation of FAK in cellular assays and an extremely high cooperativity α factor of 104, and was crystallised in complex with VHL and FAK. The ternary structure reveals several neo-PPIs between VHL and FAK (**Figure 5h**), including both H-bonds and salt bridges. Interestingly, a large interaction surface area in the ternary complex is contributed by the sandwiching of the VHL ligand between VHL and the α D helix in the C-lobe of FAK. The phenyl ring of the VHL ligand sits in a hydrophobic pocket formed by the peptide backbone between Q512 and V513 of the α D helix.

Concluding Remarks

The biochemical and structural investigations of E3 ligases continue to bear fruit and reveal expanding modes of recognition. They provide insight into how substrates and neo-substrates can be recruited, ubiquitinated, and then degraded. They also reveal how small molecules can bridge substrate and ligase to induce interactions through diverse orientations, geometries, and with distinct thermodynamic and kinetic features. The original molecular glue degraders discovered and characterized so far are monovalent and so strictly require a high-level of cooperativity to glue complexes favourably for productive ubiquitination. The discovery and structural understanding that bivalent PROTACs also exhibit high propensity to glue neo-substrates to E3 ligases have revealed how differences in molecular recognition can be exploited to drive productive ubiquitination and rapid and efficient target degradation. The mechanism of enhancing proximity and inducing protein-protein interactions between proteins is emerging as much more prevalent than previously anticipated. This realisation may have important functional and mechanistic implications that can be exploited to target other enzyme systems beyond E3 ligases.

Figure Legends

Figure 1 Native activity and pharmacological hijacking of E3 ligases. Graphical representation of natural (a), molecular glue-induced (b), and PROTAC-induced protein degradation (c) by the ubiquitin-proteasome system.

Figure 2 Types of substrate recognition by E3 ligases. Graphical representation of type 1, type 2, and type 3 substrate recognition. Modification of either the substrate (type 2), or the E3 ligase (type 3) may be either allosteric or interfacial. The modification may be covalent or non-covalent, or a proteolytic cleavage event.

Figure 3 Recognition of substrates by E3 ligases in nature. Substrate receptors and substrates are coloured grey and tan, respectively. Hydrogen bonds and the ionic interactions are represented as black dotted lines. (a) X-ray crystal structure of substrate receptor KLHL12 in complex with substrate DVL1 peptide (PDB code: 6TTK). The PGXPP motif residues of DVL1 are labelled along with Tyr512 that forms a hydrogen bond with Pro658 of the peptide. Hydrophobic residues of KLHL12 lining the binding pocket are shown as sticks. (b) X-ray crystal structure of substrate receptor GID4 in complex with substrate Pro/N-degron PGLW tetrapeptide (PDB code: 6CDC). Residues forming the hydrogen bonding network between GID4 and the N-terminal proline residue of the tetrapeptide are labelled. (c) X-ray crystal structure of substrate receptor KLHDC2 in complex with substrate SelK C-end degron peptide (PDB code: 6DO3). Residues involved in the interactions with the carboxy terminus (G91) of the SelK peptide are labelled (d) X-ray crystal structure of substrate receptor SOCS2 in complex with substrate EpoR phosphodegron peptide (PDB code: 6I4X). Hydrogen bonding and ionic interactions

between residues of SOCS2 that interact with the phosphor group of the phosphorylated tyrosine (pTyr) residue of the EpoR peptide are shown. (e) X-ray crystal structure of substrate receptor VHL in complex with substrate HIF1 α oxygen-dependent degron peptide (PDB code: 1LM8). Hydrogen bonding interactions between residues of VHL that interact with the hydroxyl group of the hydroxylated proline (HyP564) of HIF1 α are shown. (f) Cryo-EM structure of substrate receptor FBXL5 (only the substrate-interacting interface and lid loops are shown for clarity) in complex with [2Fe2S]²⁺ cluster (stick representation) and substrate IRP2 domain IV (PDB code: 6VCD). [2Fe2S]²⁺ cluster-coordinating cysteine residues are labelled and residues of FBXL5 that interact with IRP2 are shown as sticks. (g) X-ray crystal structure of substrate receptor TIR1 in complex with small molecule hormone Auxin (sphere representation, chemical structure depicted) and substrate IAA7 peptide (PDB code: 2P1Q). Auxin binding creates a new molecular surface that interacts with Trp5 and Pro 7 of the IAAP peptide (labelled).

Figure 4 Ternary co-crystal structures of molecular glue degraders (orange, chemical structure depicted) bound to E3 ligases (grey) and neo-substrates (tan). (a) X-ray crystal structure of substrate receptor CRBN in complex with molecular glue (*S*)-5-hydroxythalidomide and neo-substrate SALL4 (PDB code: 7BQV). Zinc-coordinating residues of SALL4 shown as sticks and zinc ion shown as a sphere (b) X-ray crystal structure of substrate receptor DCAF15 in complex with molecular glue indisulam and neo-substrate RBM39 (PDB code: 6UD7). (c) X-ray crystal structure of substrate receptor β -TRCP in complex with molecular glue NR2663 and substrate β -catenin peptide (PDB code: 6M92). Residues pSer33, Ile35 and Ser37 of the β -catenin peptide are shown as sticks and labelled. (d) X-ray crystal structure of adaptor protein DDB1 in complex with molecular glue and neo-substrate receptor CDK12 (PDB code: 6TD3).

Figure 5 Ternary complex co-crystal structures of heterobifunctional PROTAC degraders (orange, chemical structure depicted) bound to E3 ligases and neo-substrate targets. (a) X-ray crystal structure of ternary complex of neo-substrate BRD4, the PROTAC MZ1, and substrate receptor VHL (PDB code: 5T35). (b) X-ray crystal structure of ternary complex of neo-substrate BRD4, MacroPROTAC-1, and substrate receptor VHL (PDB code: 6SIS). (c) X-ray crystal structure of ternary complex of neo-substrate SMARCA2, PROTAC 2, and substrate receptor VHL (PDB code: 6HAX). (d) X-ray crystal structure of ternary complex of neo-substrate BRD4, the PROTAC dBET23, and substrate receptor CRBN (PDB code: 6BN7). (e) X-ray crystal structure of ternary complex of neo-substrate BCL-X_L, PROTAC6, and substrate receptor VHL (PDB code: 6ZHC). (f) X-ray crystal structure of ternary complex of neo-substrate BTK, the PROTAC BCPyr, and substrate receptor CIAP^{BIR3} (PDB code: 6W70). (g) X-ray crystal structure of ternary complex of neo-substrate BRD4, the PROTAC Compound 9, and substrate receptor VHL (PDB code: 7KHH). (h) X-ray crystal structure of ternary complex of neo-substrate FAK, the GSK215, and substrate receptor VHL (PDB code: 7PI4).

Table Legends

Table 1 Buried surface area of molecular glue and PROTAC ternary complexes. Buried surface area of the interfaces involved in the ternary complex were calculated with PISA (84).

Table S1 Extended, heading-sortable table of ternary complex interface and assembly properties in molecular glue and PROTAC ternary complex structures. Interface and assembly properties were calculated in PISA (84). Headings contain hyperlinks where an explanation of terms is necessary. Complexation significance score (CSS) from the interface module of PISA has been excluded due to the influence of adaptor proteins and other non-target, non-substrate receptor components (e.g. adaptor proteins) on the assembly term of the CSS in some structures.

Literature Cited

1. Lecker SH, Goldberg AL, Mitch WE. 2006. Protein degradation by the ubiquitin-proteasome pathway in normal and disease states. *J Am Soc Nephrol* 17: 1807-19
2. Komander D, Rape M. 2012. The ubiquitin code. *Annu Rev Biochem* 81: 203-29
3. Zheng N, Shabek N. 2017. Ubiquitin Ligases: Structure, Function, and Regulation. *Annu Rev Biochem* 86: 129-57
4. Morreale FE, Walden H. 2016. Types of Ubiquitin Ligases. *Cell* 165: 248-48 e1
5. Petroski MD, Deshaies RJ. 2005. Function and regulation of cullin-RING ubiquitin ligases. *Nat Rev Mol Cell Biol* 6: 9-20
6. Bulatov E, Ciulli A. 2015. Targeting Cullin-RING E3 ubiquitin ligases for drug discovery: structure, assembly and small-molecule modulation. *Biochem J* 467: 365-86
7. Lorenz S. 2018. Structural mechanisms of HECT-type ubiquitin ligases. *Biol Chem* 399: 127-45
8. Weber J, Polo S, Maspero E. 2019. HECT E3 Ligases: A Tale With Multiple Facets. *Front Physiol* 10: 370
9. Cotton TR, Lechtenberg BC. 2020. Chain reactions: molecular mechanisms of RBR ubiquitin ligases. *Biochem Soc Trans* 48: 1737-50
10. Haakonsen DL, Rape M. 2019. Branching Out: Improved Signaling by Heterotypic Ubiquitin Chains. *Trends Cell Biol* 29: 704-16
11. French ME, Koehler CF, Hunter T. 2021. Emerging functions of branched ubiquitin chains. *Cell Discov* 7: 6
12. Swatek KN, Komander D. 2016. Ubiquitin modifications. *Cell Res* 26: 399-422
13. Nalepa G, Rolfe M, Harper JW. 2006. Drug discovery in the ubiquitin-proteasome system. *Nat Rev Drug Discov* 5: 596-613
14. Wertz IE, Wang X. 2019. From Discovery to Bedside: Targeting the Ubiquitin System. *Cell Chem Biol* 26: 156-77
15. Huang X, Dixit VM. 2016. Drugging the undruggables: exploring the ubiquitin system for drug development. *Cell Res* 26: 484-98
16. Bondeson DP, Crews CM. 2017. Targeted Protein Degradation by Small Molecules. *Annu Rev Pharmacol Toxicol* 57: 107-23
17. Zhou P, Bogacki R, McReynolds L, Howley PM. 2000. Harnessing the ubiquitination machinery to target the degradation of specific cellular proteins. *Mol Cell* 6: 751-6

18. Sakamoto KM, Kim KB, Kumagai A, Mercurio F, Crews CM, Deshaies RJ. 2001. Protacs: chimeric molecules that target proteins to the Skp1-Cullin-F box complex for ubiquitination and degradation. *Proc Natl Acad Sci U S A* 98: 8554-9
19. Schneekloth JS, Jr., Fonseca FN, Koldobskiy M, Mandal A, Deshaies R, et al. 2004. Chemical genetic control of protein levels: selective in vivo targeted degradation. *J Am Chem Soc* 126: 3748-54
20. Winter GE, Buckley DL, Paulk J, Roberts JM, Souza A, et al. 2015. DRUG DEVELOPMENT. Phthalimide conjugation as a strategy for in vivo target protein degradation. *Science* 348: 1376-81
21. Deshaies RJ. 2015. Protein degradation: Prime time for PROTACs. *Nat Chem Biol* 11: 634-5
22. Bondeson DP, Mares A, Smith IE, Ko E, Campos S, et al. 2015. Catalytic in vivo protein knockdown by small-molecule PROTACs. *Nat Chem Biol* 11: 611-7
23. Lu J, Qian Y, Altieri M, Dong H, Wang J, et al. 2015. Hijacking the E3 Ubiquitin Ligase Cereblon to Efficiently Target BRD4. *Chem Biol* 22: 755-63
24. Zengerle M, Chan KH, Ciulli A. 2015. Selective Small Molecule Induced Degradation of the BET Bromodomain Protein BRD4. *ACS Chem Biol* 10: 1770-7
25. Mullard A. 2021. Targeted protein degraders crowd into the clinic. *Nat Rev Drug Discov* 20: 247-50
26. Alabi SB, Crews CM. 2021. Major advances in targeted protein degradation: PROTACs, LYTACs, and MADTACs. *J Biol Chem* 296: 100647
27. Roth S, Fulcher LJ, Sapkota GP. 2019. Advances in targeted degradation of endogenous proteins. *Cell Mol Life Sci* 76: 2761-77
28. Harper JW, Schulman BA. 2021. Cullin-RING Ubiquitin Ligase Regulatory Circuits: A Quarter Century Beyond the F-Box Hypothesis. *Annu Rev Biochem* 90: 403-29
29. Angers S, Thorpe CJ, Biechele TL, Goldenberg SJ, Zheng N, et al. 2006. The KLHL12-Cullin-3 ubiquitin ligase negatively regulates the Wnt-beta-catenin pathway by targeting Dishevelled for degradation. *Nat Cell Biol* 8: 348-57
30. Funato Y, Terabayashi T, Sakamoto R, Okuzaki D, Ichise H, et al. 2010. Nucleoredoxin sustains Wnt/beta-catenin signaling by retaining a pool of inactive dishevelled protein. *Curr Biol* 20: 1945-52
31. Shami Shah A, Batrouni AG, Kim D, Punyala A, Cao W, et al. 2019. PLEKHA4/kramer Attenuates Dishevelled Ubiquitination to Modulate Wnt and Planar Cell Polarity Signaling. *Cell Rep* 27: 2157-70 e8
32. Zhao B, Payne WG, Sai J, Lu Z, Olejniczak ET, Fesik SW. 2020. Structural Elucidation of Peptide Binding to KLHL-12, a Substrate Specific Adapter Protein in a Cul3-Ring E3 Ligase Complex. *Biochemistry* 59: 964-69

33. Chen Z, Wasney GA, Picaud S, Filippakopoulos P, Vedadi M, et al. 2020. Identification of a PGXPP degron motif in dishevelled and structural basis for its binding to the E3 ligase KLHL12. *Open Biol* 10: 200041
34. de Brevern AG. 2016. Extension of the classical classification of beta-turns. *Sci Rep* 6: 33191
35. Chen Z, Picaud S, Filippakopoulos P, D'Angiolella V, Bullock AN. 2019. Structural Basis for Recruitment of DAPK1 to the KLHL20 E3 Ligase. *Structure* 27: 1395-404 e4
36. Zhuang M, Calabrese MF, Liu J, Waddell MB, Nourse A, et al. 2009. Structures of SPOP-substrate complexes: insights into molecular architectures of BTB-Cul3 ubiquitin ligases. *Mol Cell* 36: 39-50
37. Ostertag MS, Messias AC, Sattler M, Popowicz GM. 2019. The Structure of the SPOP-Pdx1 Interface Reveals Insights into the Phosphorylation-Dependent Binding Regulation. *Structure* 27: 327-34 e3
38. Lumpkin RJ, Baker RW, Leschziner AE, Komives EA. 2020. Structure and dynamics of the ASB9 CUL-RING E3 Ligase. *Nat Commun* 11: 2866
39. Varshavsky A. 2019. N-degron and C-degron pathways of protein degradation. *Proc Natl Acad Sci U S A* 116: 358-66
40. Timms RT, Koren I. 2020. Tying up loose ends: the N-degron and C-degron pathways of protein degradation. *Biochem Soc Trans* 48: 1557-67
41. Santt O, Pfirrmann T, Braun B, Juretschke J, Kimmig P, et al. 2008. The yeast GID complex, a novel ubiquitin ligase (E3) involved in the regulation of carbohydrate metabolism. *Molecular Biology of the Cell* 19: 3323-33
42. Hammerle M, Bauer J, Rose M, Szallies A, Thumm M, et al. 1998. Proteins of newly isolated mutants and the amino-terminal proline are essential for ubiquitin-proteasome-catalyzed catabolite degradation of fructose-1,6-bisphosphatase of *Saccharomyces cerevisiae*. *Journal of Biological Chemistry* 273: 25000-05
43. Chen SJ, Wu X, Wadas B, Oh JH, Varshavsky A. 2017. An N-end rule pathway that recognizes proline and destroys gluconeogenic enzymes. *Science* 355
44. Xiao Q, Zhang FR, Nacev BA, Liu JO, Pei DH. 2010. Protein N-Terminal Processing: Substrate Specificity of *Escherichia coli* and Human Methionine Aminopeptidases. *Biochemistry* 49: 5588-99
45. Dong C, Zhang H, Li L, Tempel W, Loppnau P, Min J. 2018. Molecular basis of GID4-mediated recognition of degrons for the Pro/N-end rule pathway. *Nat Chem Biol* 14: 466-73
46. Koren I, Timms RT, Kula T, Xu Q, Li MZ, Elledge SJ. 2018. The Eukaryotic Proteome Is Shaped by E3 Ubiquitin Ligases Targeting C-Terminal Degrons. *Cell* 173: 1622-35 e14
47. Rusnac DV, Lin HC, Canzani D, Tien KX, Hinds TR, et al. 2018. Recognition of the Diglycine C-End Degron by CRL2(KLHDC2) Ubiquitin Ligase. *Mol Cell* 72: 813-22 e4

48. Kershaw NJ, Murphy JM, Liao NP, Varghese LN, Laktyushin A, et al. 2013. SOCS3 binds specific receptor-JAK complexes to control cytokine signaling by direct kinase inhibition. *Nat Struct Mol Biol* 20: 469-76
49. Liao NPD, Laktyushin A, Lucet IS, Murphy JM, Yao S, et al. 2018. The molecular basis of JAK/STAT inhibition by SOCS1. *Nat Commun* 9: 1558
50. Zadjali F, Pike AC, Vesterlund M, Sun J, Wu C, et al. 2011. Structural basis for c-KIT inhibition by the suppressor of cytokine signaling 6 (SOCS6) ubiquitin ligase. *J Biol Chem* 286: 480-90
51. Kung WW, Ramachandran S, Makukhin N, Bruno E, Ciulli A. 2019. Structural insights into substrate recognition by the SOCS2 E3 ubiquitin ligase. *Nat Commun* 10: 2534
52. Ivan M, Kondo K, Yang H, Kim W, Valiando J, et al. 2001. HIF α targeted for VHL-mediated destruction by proline hydroxylation: implications for O₂ sensing. *Science* 292: 464-8
53. Jaakkola P, Mole DR, Tian YM, Wilson MI, Gielbert J, et al. 2001. Targeting of HIF- α to the von Hippel-Lindau ubiquitylation complex by O₂-regulated prolyl hydroxylation. *Science* 292: 468-72
54. Min JH, Yang H, Ivan M, Gertler F, Kaelin WG, Jr., Pavletich NP. 2002. Structure of an HIF-1 α -pVHL complex: hydroxyproline recognition in signaling. *Science* 296: 1886-9
55. Hon WC, Wilson MI, Harlos K, Claridge TD, Schofield CJ, et al. 2002. Structural basis for the recognition of hydroxyproline in HIF-1 α by pVHL. *Nature* 417: 975-8
56. Galdeano C, Gadd MS, Soares P, Scaffidi S, Van Molle I, et al. 2014. Structure-guided design and optimization of small molecules targeting the protein-protein interaction between the von Hippel-Lindau (VHL) E3 ubiquitin ligase and the hypoxia inducible factor (HIF) α subunit with in vitro nanomolar affinities. *J Med Chem* 57: 8657-63
57. Frost J, Galdeano C, Soares P, Gadd MS, Grzes KM, et al. 2016. Potent and selective chemical probe of hypoxic signalling downstream of HIF- α hydroxylation via VHL inhibition. *Nat Commun* 7: 13312
58. Guo B, Phillips JD, Yu Y, Leibold EA. 1995. Iron regulates the intracellular degradation of iron regulatory protein 2 by the proteasome. *J Biol Chem* 270: 21645-51
59. Haile DJ, Rouault TA, Harford JB, Kennedy MC, Blondin GA, et al. 1992. Cellular regulation of the iron-responsive element binding protein: disassembly of the cubane iron-sulfur cluster results in high-affinity RNA binding. *Proc Natl Acad Sci U S A* 89: 11735-9
60. Hanson ES, Foot LM, Leibold EA. 1999. Hypoxia post-translationally activates iron-regulatory protein 2. *J Biol Chem* 274: 5047-52
61. Hanson ES, Rawlins ML, Leibold EA. 2003. Oxygen and iron regulation of iron regulatory protein 2. *J Biol Chem* 278: 40337-42
62. Iwai K, Klausner RD, Rouault TA. 1995. Requirements for iron-regulated degradation of the RNA binding protein, iron regulatory protein 2. *EMBO J* 14: 5350-7

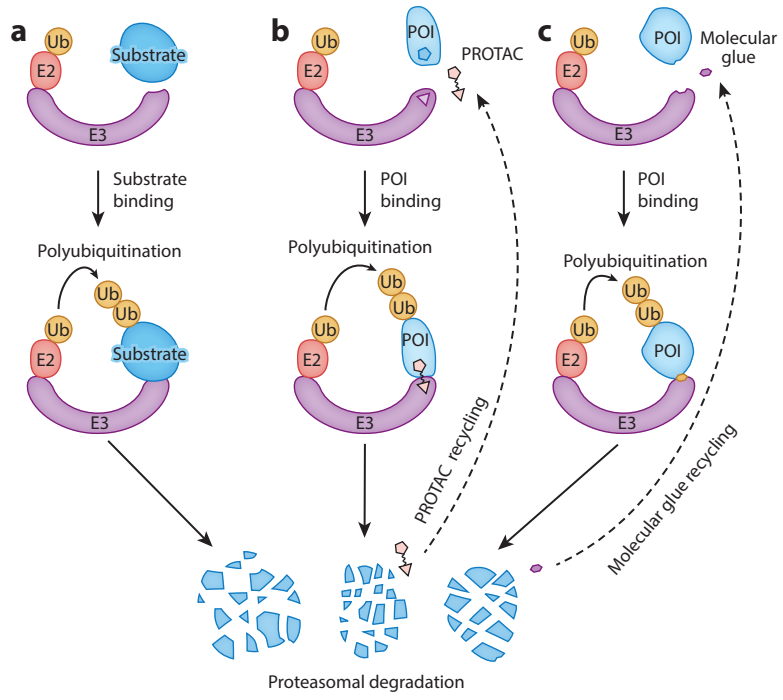
63. Salahudeen AA, Thompson JW, Ruiz JC, Ma HW, Kinch LN, et al. 2009. An E3 ligase possessing an iron-responsive hemerythrin domain is a regulator of iron homeostasis. *Science* 326: 722-6
64. Vashisht AA, Zumbrennen KB, Huang X, Powers DN, Durazo A, et al. 2009. Control of iron homeostasis by an iron-regulated ubiquitin ligase. *Science* 326: 718-21
65. Wang H, Shi H, Rajan M, Canarie ER, Hong S, et al. 2020. FBXL5 Regulates IRP2 Stability in Iron Homeostasis via an Oxygen-Responsive [2Fe2S] Cluster. *Mol Cell* 78: 31-41 e5
66. Thompson JW, Salahudeen AA, Chollangi S, Ruiz JC, Brautigam CA, et al. 2012. Structural and molecular characterization of iron-sensing hemerythrin-like domain within F-box and leucine-rich repeat protein 5 (FBXL5). *J Biol Chem* 287: 7357-65
67. Tan X, Calderon-Villalobos LI, Sharon M, Zheng C, Robinson CV, et al. 2007. Mechanism of auxin perception by the TIR1 ubiquitin ligase. *Nature* 446: 640-5
68. Sheard LB, Tan X, Mao H, Withers J, Ben-Nissan G, et al. 2010. Jasmonate perception by inositol-phosphate-potentiated COI1-JAZ co-receptor. *Nature* 468: 400-5
69. Che Y, Gilbert AM, Shanmugasundaram V, Noe MC. 2018. Inducing protein-protein interactions with molecular glues. *Bioorg Med Chem Lett* 28: 2585-92
70. Schreiber SL. 2021. The Rise of Molecular Glues. *Cell* 184: 3-9
71. Vargesson N. 2015. Thalidomide-induced teratogenesis: history and mechanisms. *Birth Defects Res C Embryo Today* 105: 140-56
72. Ito T, Ando H, Suzuki T, Ogura T, Hotta K, et al. 2010. Identification of a primary target of thalidomide teratogenicity. *Science* 327: 1345-50
73. Chamberlain PP, Lopez-Girona A, Miller K, Carmel G, Pagarigan B, et al. 2014. Structure of the human Cereblon-DDB1-lenalidomide complex reveals basis for responsiveness to thalidomide analogs. *Nat Struct Mol Biol* 21: 803-9
74. Fischer ES, Bohm K, Lydeard JR, Yang H, Stadler MB, et al. 2014. Structure of the DDB1-CRBN E3 ubiquitin ligase in complex with thalidomide. *Nature* 512: 49-53
75. Lu G, Middleton RE, Sun H, Naniong M, Ott CJ, et al. 2014. The myeloma drug lenalidomide promotes the cereblon-dependent destruction of Ikaros proteins. *Science* 343: 305-9
76. Kronke J, Udeshi ND, Narla A, Grauman P, Hurst SN, et al. 2014. Lenalidomide causes selective degradation of IKZF1 and IKZF3 in multiple myeloma cells. *Science* 343: 301-5
77. Matyskiela ME, Clayton T, Zheng X, Mayne C, Tran E, et al. 2020. Crystal structure of the SALL4-pomalidomide-cereblon-DDB1 complex. *Nat Struct Mol Biol* 27: 319-22
78. Sievers QL, Petzold G, Bunker RD, Renneville A, Slabicki M, et al. 2018. Defining the human C2H2 zinc finger degrome targeted by thalidomide analogs through CRBN. *Science* 362

79. Uehara T, Minoshima Y, Sagane K, Sugi NH, Mitsuhashi KO, et al. 2017. Selective degradation of splicing factor CAPERalpha by anticancer sulfonamides. *Nat Chem Biol* 13: 675-80
80. Han T, Goralski M, Gaskill N, Capota E, Kim J, et al. 2017. Anticancer sulfonamides target splicing by inducing RBM39 degradation via recruitment to DCAF15. *Science* 356
81. Du X, Volkov OA, Czerwinski RM, Tan H, Huerta C, et al. 2019. Structural Basis and Kinetic Pathway of RBM39 Recruitment to DCAF15 by a Sulfonamide Molecular Glue E7820. *Structure* 27: 1625-33 e3
82. Faust TB, Yoon H, Nowak RP, Donovan KA, Li Z, et al. 2020. Structural complementarity facilitates E7820-mediated degradation of RBM39 by DCAF15. *Nat Chem Biol* 16: 7-14
83. Bussiere DE, Xie L, Srinivas H, Shu W, Burke A, et al. 2020. Structural basis of indisulam-mediated RBM39 recruitment to DCAF15 E3 ligase complex. *Nat Chem Biol* 16: 15-23
84. 'Protein interfaces, surfaces and assemblies' service PISA at the European Bioinformatics Institute. (http://www.ebi.ac.uk/pdbe/prot_int/pistart.html).
85. Krissinel E, Henrick K. 2007. Inference of macromolecular assemblies from crystalline state. *J Mol Biol* 372: 774-97
86. Aberle H, Bauer A, Stappert J, Kispert A, Kemler R. 1997. beta-catenin is a target for the ubiquitin-proteasome pathway. *EMBO J* 16: 3797-804
87. Kitagawa M, Hatakeyama S, Shirane M, Matsumoto M, Ishida N, et al. 1999. An F-box protein, FWD1, mediates ubiquitin-dependent proteolysis of beta-catenin. *EMBO J* 18: 2401-10
88. Rubinfeld B, Robbins P, El-Gamil M, Albert I, Porfiri E, Polakis P. 1997. Stabilization of beta-catenin by genetic defects in melanoma cell lines. *Science* 275: 1790-2
89. Polakis P. 2012. Wnt signaling in cancer. *Cold Spring Harb Perspect Biol* 4
90. Simonetta KR, Taygerly J, Boyle K, Basham SE, Padovani C, et al. 2019. Prospective discovery of small molecule enhancers of an E3 ligase-substrate interaction. *Nat Commun* 10: 1402
91. Slabicki M, Kozicka Z, Petzold G, Li YD, Manojkumar M, et al. 2020. The CDK inhibitor CR8 acts as a molecular glue degrader that depletes cyclin K. *Nature* 585: 293-97
92. Mayor-Ruiz C, Bauer S, Brand M, Kozicka Z, Siklos M, et al. 2020. Rational discovery of molecular glue degraders via scalable chemical profiling. *Nat Chem Biol* 16: 1199-207
93. Lv L, Chen P, Cao L, Li Y, Zeng Z, et al. 2020. Discovery of a molecular glue promoting CDK12-DDB1 interaction to trigger cyclin K degradation. *Elife* 9
94. Slabicki M, Yoon H, Koeppel J, Nitsch L, Roy Burman SS, et al. 2020. Small-molecule-induced polymerization triggers degradation of BCL6. *Nature* 588: 164-68
95. Pettersson M, Crews CM. 2019. PROteolysis TARgeting Chimeras (PROTACs) - Past, present and future. *Drug Discov Today Technol* 31: 15-27

96. Sun X, Gao H, Yang Y, He M, Wu Y, et al. 2019. PROTACs: great opportunities for academia and industry. *Signal Transduct Target Ther* 4: 64
97. Verma R, Mohl D, Deshaies RJ. 2020. Harnessing the Power of Proteolysis for Targeted Protein Inactivation. *Mol Cell* 77: 446-60
98. Ishida T, Ciulli A. 2021. E3 Ligase Ligands for PROTACs: How They Were Found and How to Discover New Ones. *SLAS Discov* 26: 484-502
99. Gadd MS, Testa A, Lucas X, Chan KH, Chen W, et al. 2017. Structural basis of PROTAC cooperative recognition for selective protein degradation. *Nat Chem Biol* 13: 514-21
100. Roy MJ, Winkler S, Hughes SJ, Whitworth C, Galant M, et al. 2019. SPR-Measured Dissociation Kinetics of PROTAC Ternary Complexes Influence Target Degradation Rate. *ACS Chem Biol* 14: 361-68
101. Bondeson DP, Smith BE, Burslem GM, Buhimschi AD, Hines J, et al. 2018. Lessons in PROTAC Design from Selective Degradation with a Promiscuous Warhead. *Cell Chem Biol* 25: 78-87 e5
102. Baratta MG, Schinzel AC, Zwang Y, Bandopadhyay P, Bowman-Colin C, et al. 2015. An in-tumor genetic screen reveals that the BET bromodomain protein, BRD4, is a potential therapeutic target in ovarian carcinoma. *Proc Natl Acad Sci U S A* 112: 232-7
103. Fujisawa T, Filippakopoulos P. 2017. Functions of bromodomain-containing proteins and their roles in homeostasis and cancer. *Nat Rev Mol Cell Biol* 18: 246-62
104. Testa A, Hughes SJ, Lucas X, Wright JE, Ciulli A. 2020. Structure-Based Design of a Macrocyclic PROTAC. *Angew Chem Int Ed Engl* 59: 1727-34
105. Farnaby W, Koegl M, Roy MJ, Whitworth C, Diers E, et al. 2019. BAF complex vulnerabilities in cancer demonstrated via structure-based PROTAC design. *Nat Chem Biol* 15: 672-80
106. Sutherland CL, Tallant C, Monteiro OP, Yapp C, Fuchs JE, et al. 2016. Identification and Development of 2,3-Dihydropyrrolo[1,2-a]quinazolin-5(1H)-one Inhibitors Targeting Bromodomains within the Switch/Sucrose Nonfermenting Complex. *J Med Chem* 59: 5095-101
107. Myrianthopoulos V, Gaboriaud-Kolar N, Tallant C, Hall ML, Grigoriou S, et al. 2016. Discovery and Optimization of a Selective Ligand for the Switch/Sucrose Nonfermenting-Related Bromodomains of Polybromo Protein-1 by the Use of Virtual Screening and Hydration Analysis. *J Med Chem* 59: 8787-803
108. Soares P, Gadd MS, Frost J, Galdeano C, Ellis L, et al. 2018. Group-Based Optimization of Potent and Cell-Active Inhibitors of the von Hippel-Lindau (VHL) E3 Ubiquitin Ligase: Structure-Activity Relationships Leading to the Chemical Probe (2S,4R)-1-((S)-2-(1-Cyanocyclopropanecarboxamido)-3,3-dimethylbutanoyl)-4-hydroxy -N-(4-(4-methylthiazol-5-yl)benzyl)pyrrolidine-2-carboxamide (VH298). *J Med Chem* 61: 599-618
109. Chan KH, Zengerle M, Testa A, Ciulli A. 2018. Impact of Target Warhead and Linkage Vector on Inducing Protein Degradation: Comparison of Bromodomain and Extra-Terminal (BET)

- Degraders Derived from Triazolodiazepine (JQ1) and Tetrahydroquinoline (I-BET726) BET Inhibitor Scaffolds. *J Med Chem* 61: 504-13
110. Nowak RP, DeAngelo SL, Buckley D, He Z, Donovan KA, et al. 2018. Plasticity in binding confers selectivity in ligand-induced protein degradation. *Nat Chem Biol* 14: 706-14
 111. Douglass EF, Jr., Miller CJ, Sparer G, Shapiro H, Spiegel DA. 2013. A comprehensive mathematical model for three-body binding equilibria. *J Am Chem Soc* 135: 6092-9
 112. Chung CW, Dai H, Fernandez E, Tinworth CP, Churcher I, et al. 2020. Structural Insights into PROTAC-Mediated Degradation of Bcl-xL. *ACS Chem Biol* 15: 2316-23
 113. Adams JM, Cory S. 2018. The BCL-2 arbiters of apoptosis and their growing role as cancer targets. *Cell Death Differ* 25: 27-36
 114. Perini GF, Ribeiro GN, Pinto Neto JV, Campos LT, Hamerschlak N. 2018. BCL-2 as therapeutic target for hematological malignancies. *J Hematol Oncol* 11: 65
 115. Mason KD, Carpinelli MR, Fletcher JI, Collinge JE, Hilton AA, et al. 2007. Programmed anuclear cell death delimits platelet life span. *Cell* 128: 1173-86
 116. He Y, Koch R, Budamagunta V, Zhang P, Zhang X, et al. 2020. DT2216-a Bcl-xL-specific degrader is highly active against Bcl-xL-dependent T cell lymphomas. *J Hematol Oncol* 13: 95
 117. Tao ZF, Hasvold L, Wang L, Wang X, Petros AM, et al. 2014. Discovery of a Potent and Selective BCL-XL Inhibitor with in Vivo Activity. *ACS Med Chem Lett* 5: 1088-93
 118. Dragovich PS, Pillow TH, Blake RA, Sadowsky JD, Adaligil E, et al. 2021. Antibody-Mediated Delivery of Chimeric BRD4 Degraders. Part 1: Exploration of Antibody Linker, Payload Loading, and Payload Molecular Properties. *J Med Chem* 64: 2534-75
 119. Dragovich PS, Pillow TH, Blake RA, Sadowsky JD, Adaligil E, et al. 2021. Antibody-Mediated Delivery of Chimeric BRD4 Degraders. Part 2: Improvement of In Vitro Antiproliferation Activity and In Vivo Antitumor Efficacy. *J Med Chem* 64: 2576-607
 120. Law RP, Nunes J, Chung CW, Bantscheff M, Buda K, et al. 2021. Discovery and Characterisation of Highly Cooperative FAK-Degrading PROTACs. *Angew Chem Int Ed Engl* 60: 23327-34
 121. Sulzmaier FJ, Jean C, Schlaepfer DD. 2014. FAK in cancer: mechanistic findings and clinical applications. *Nat Rev Cancer* 14: 598-610
 122. Golubovskaya VM, Kweh FA, Cance WG. 2009. Focal adhesion kinase and cancer. *Histol Histopathol* 24: 503-10
 123. Cromm PM, Samarasinghe KTG, Hines J, Crews CM. 2018. Addressing Kinase-Independent Functions of Fak via PROTAC-Mediated Degradation. *J Am Chem Soc* 140: 17019-26
 124. Popow J, Arnhof H, Bader G, Berger H, Ciulli A, et al. 2019. Highly Selective PTK2 Proteolysis Targeting Chimeras to Probe Focal Adhesion Kinase Scaffolding Functions. *J Med Chem* 62: 2508-20

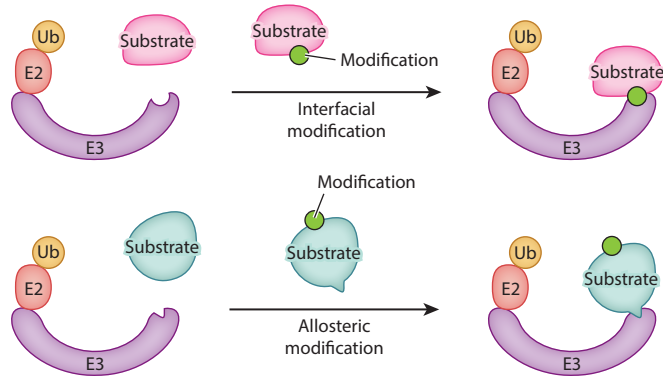
125. Gao HY, Wu Y, Sun YH, Yang YQ, Zhou GB, Rao Y. 2020. Design, Synthesis, and Evaluation of Highly Potent FAK-Targeting PROTACs. *Acs Medicinal Chemistry Letters* 11: 1855-62
126. Kargbo RB. 2020. Chemically Induced Degradation of FAK-ALK for Application in Cancer Therapeutics. *ACS Med Chem Lett* 11: 1367-68
127. Kargbo RB. 2020. Bifunctional Pyrimidines as Modulators of Focal Adhesion Kinase. *ACS Med Chem Lett* 11: 409-11
128. Gao HY, Zheng CW, Du J, Wu Y, Sun YH, et al. 2020. FAK-targeting PROTAC as a chemical tool for the investigation of non-enzymatic FAK function in mice. *Protein & Cell* 11: 534-39
129. Tanjoni I, Walsh C, Uryu S, Tomar A, Nam JO, et al. 2010. PND-1186 FAK inhibitor selectively promotes tumor cell apoptosis in three-dimensional environments. *Cancer Biol Ther* 9: 764-77
130. Raina K, Lu J, Qian Y, Altieri M, Gordon D, et al. 2016. PROTAC-induced BET protein degradation as a therapy for castration-resistant prostate cancer. *Proc Natl Acad Sci U S A* 113: 7124-9



a Type 1 substrate recognition



b Type 2 substrate recognition



c Type 3 substrate recognition

